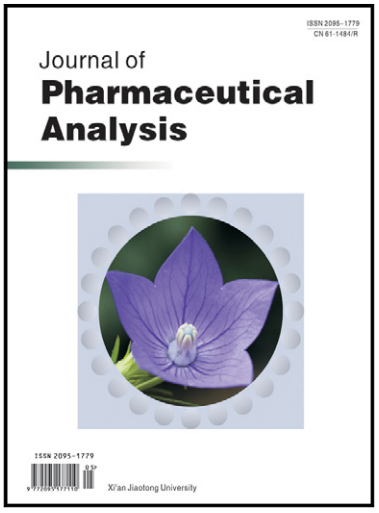

Synthesis of carbon nano sheet from barley and its use as non enzymatic glucose biosensor

Soma Das, Mitali Saha

PII: S2095-1779(14)00012-4
DOI: http://dx.doi.org/10.1016/j.jpha.2014.03.004
Reference: JPHA215

www.elsevier.com/locate/jpa
www.sciencedirect.com

To appear in: *Journal of Pharmaceutical Analysis*

Received date: 5 November 2013
Revised date: 5 March 2014
Accepted date: 11 March 2014

Cite this article as: Soma Das, Mitali Saha, Synthesis of carbon nano sheet from barley and its use as non enzymatic glucose biosensor, *Journal of Pharmaceutical Analysis,* http://dx.doi.org/10.1016/j.jpha.2014.03.004

Synthesis of carbon nano sheet from barley and its use as non enzymatic glucose biosensor

Short Title : Non enzymatic glucose biosensor

Soma Das and Mitali Saha*

Department of Chemistry, National Institute of Technology, Agartala-799046, Tripura, India

Abstract

In this work, carbon nano sheet (CNS) based electrode was designed for electrochemical biosensing of glucose. CNS has been obtained by the pyrolysis of barley at 600-750^{o}C in a muffle furnace, which was then purified and functionalized. The CNS has been characterized by scanning electron microscopy (SEM), X-ray diffraction (XRD) and Raman spectroscopic techniques. The electrochemical activity of CNS based electrode was investigated by linear sweep voltammetry (LSV) and square wave voltammetry (SWV), for the oxidation of glucose in 0.001 M H_2SO_4 (pH 6.0). The linear range of the sensor was found to be 10^{-4} - 10^{-6} M (1 - 100 μM) within the response time of 4s. Interestingly, its sensitivity reached as high as ~26.002 ± 0.01 μA/μM•cm^2. Electrochemical experiments revealed that the proposed electrode offered an excellent electrochemical activity towards the oxidation of glucose and could be applied for the construction of non-enzymatic glucose biosensor.

Key words: *Carbon nano sheet; β –D glucose; linear sweep voltammetry; square wave voltammetry; Pharmaceutical analysis.*

* *Corresponding author:* Email: mitalichem71@gmail.com Tel: +918974006400

1. Introduction

The continuous development of new nano materials for their applications in electroanalytical techniques, has been associated with the necessity of the improvement of the quality of efficient electrochemical devices and bio-devices. Nowadays, designing of more sensitive and selective electrochemical devices to recognize the small quantity of analytes has been received more and more attentions [1]. Carbon-based nanomaterials, especially carbon nanotubes and graphene, are extremely attractive in the bio-analytical area for electrode design as they can combine properties of the high surface area, acceptable biocompatibility, chemical and electrochemical stability and good electrical conductivity [2,3]. Furthermore, many works have shown that the application of different kinds of carbon nanomaterials is receiving more interests in electroanalytical chemistry, because of their effective surface area.

Diabetes has remained a major cause of death and serious vascular and neuropathy diseases. The diagnosis and management of diabetic patients require precise monitoring and control of the glucose level in the body. Therefore, frequent testing of the physiological glucose level is critical to confirm treatment efficiency, prevent long-term complications and avoid a diabetic emergency, such as hypoglycaemia (low blood sugar, <3 mM). This urgency has led to fascinating research and innovative detection strategies in glucose biosensor field. Electrochemical glucose biosensors had their beginning in 1962 reported by Clark and Lyons, describing the measurement of glucose in blood plasma using the enzyme glucose oxidase coupled with a potentiometric electrochemical biosensor. Electrochemical methods based on glucose oxidase (GOx) have played a vital role in simple easy-to-use blood sugar testing and

they have been widely studied over the last few decades for continuous glucose monitoring [4-12].

Enzyme-based sensors show good selectivity and high sensitivity but their activity is affected by temperature, pH, and toxic chemicals [13,14]. In order to overcome these drawbacks of enzymatic glucose sensors, nonenzymatic glucose sensors have been designed and fabricated, which have several attractive advantages, such as stability, selectivity, sensitivity, lower detection limit, etc [15-28].

In continuation of our earlier research work of synthesis of carbon nanoparticles from different natural sources [29-32], we have now used barley, which is rich in complex carbohydrates mainly starch (76%). Interestingly, it gave another nano form of carbon i.e, carbon nano-sheet (CNS), after pyrolysis at 600-750^{o}C in muffle furnace. A non enzymatic glucose biosensor was fabricated from CNS and electrochemical studies have been carried out using linear sweep voltammetry (LSV) and square wave voltammetry (SWV). The results showed that the simple preparation procedure coupled with the low cost and high electrochemical activity, unfolds a new pathway for economic, reliable and sensitive detection of glucose.

2. Experimental

2.1 Reagents

β –D glucose (99.5%) and H_2SO_4 were purchased from Sigma. All solutions were prepared with deionized water. Pyrolysis of barley was carried out in a muffle furnace (Tanco, PL Tandon & Company,India).The surface morphology of CNS was studied by a scanning electron microscope (FEI Quanta 200 Hv) and X-ray diffraction (XRD) patterns were recorded with JSO ISO DEBYEFLEX 2002 Model X-ray powder diffractometer. Raman spectra was recorded using a

Raman spectrometer; WITEC MODEL with 514 nm excitation. Electrochemical studies were performed using a mini potentiostat (Dropsens μstat 100,Spain).

2.2 Synthesis and functionalization of CNS

CNS was synthesized by pyrolyzing a cheap and readily available raw material barley, at 600-750^{o}C for 2 h under insufficient flow of air in a muffle furnace. The black carbon soot obtained was collected in a thimble and placed into a soxhlet extractor for sequential purification with petroleum ether, acetone, ethyl alcohol and finally with water followed by functionalization with nitric acid. 250 mL of 2M HNO_3 was stirred with the carbon powder for several minutes and then kept overnight. Excess nitrate was then removed by repeatedly dissolving the black particles in water and then evaporated to dryness. The powdered CNS was then characterized by SEM, XRD and Raman spectroscopy.

2.3 Fabrication of CNS electrode

The CNS electrode was fabricated following our reported method [29], just like the commercially available standard electrode DS110 (DRP 110CNT). It was fabricated on an insulating Teflon material which contains three silver wires. Both working electrode and counter electrode were made of CNS while reference electrode and electric contacts were made of silver (Fig. 1). Its dimensions is 3.5 cm × 1.0 cm × 0.5 cm (Length x Width x Height) and it is ideal for working with 50 μL volume like the standard electrode.

CNS was first stirred with polystyrene solution, prepared in chloroform (9:1 ratio) followed by sonication. A drop of the slurry was then deposited as a very fine thin film on the Teflon substrate covering two silver wires, serving as working and counter electrodes. The third silver wire was used as a reference electrode.

2.4 Non-enzymatic detection of β –D glucose with fabricated CNS electrode

For non-enzymatic detection of β –D glucose, LSV and SWV studies were carried out at CNS electrode using different concentration of glucose in 0.001 M H_2SO_4, maintaining the pH at 6.0. Then, 50μL of the glucose solution was taken by micropipette and dropped on the surface of electrode.

3. Results and discussions

3.1 Characterizations of CNS

SEM images shown in Fig. 2, clearly indicated the formation of carbon nano particles arranged in sheet like pattern, having width below 50 nm. Fig. 3 showed the XRD patterns of CNS. Two predominant peaks were observed at around 25.69^0 and 41.65^0, which were assigned for (002) and (111) reflections. Fig. 4 showed the Raman spectra of CNS with two prominent peaks at around 1310 cm^{-1} and 1620 cm^{-1}. The peak having less intensity is known as D band and peak having more intensity is known as G band.

3.2 Mechanism of non-enzymatic glucose detection at CNS electrode

It has been observed that the functionalization of CNS with 2M HNO_3 leads to the generation of functional groups like hydroxyl (-OH) and carboxyl groups (-COOH) which were suitable for ongoing derivatization reactions [33]. These groups were responsible for the adsorption of glucose molecules on the surface of carbon nanoparticles. The probable reactions are described in Scheme-1[34]. During the reaction, when β –D glucose reacts with H_2SO_4, it liberates two protons and two electrons, converting into gluconolactone and hydrogen peroxide. On further hydrolysis, the ring structure of gluconolactone breaks into open structure of gluconic acid.

$C_6H_{12}O_6$ (β –D glucose) + H_2SO_4 (0.001 M) + H_2O Gluconolactone + H_2O_2

Hydrolysis

Gluconic acid

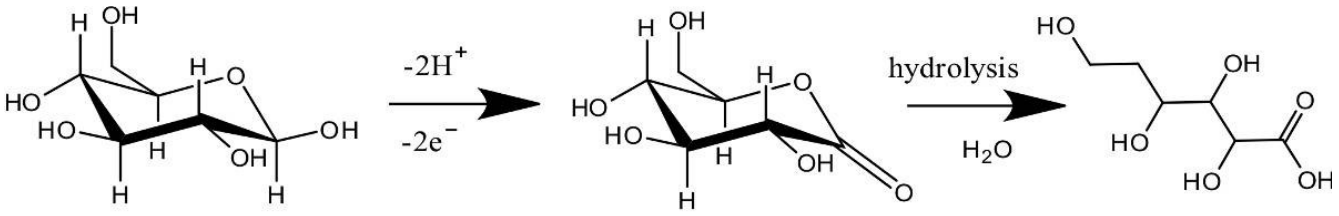

β -glucose gluconolactone gluconic acid

Scheme-1: Oxidation of β-glucose to gluconic acid

3.3 Effect of scan rate on the peak current and peak potential of β –D glucose at CNS electrode

LSV was employed to find out the effect of the scan rate on the electrochemical detection of β –D glucose at the CNS electrode. Fig. 5 displayed 2D and 3D plots of LSV, which showed the overlapping of voltagrams of 10^{-5} M β –D glucose (pH ~6.0) at various scan rates. The current versus scan rate plot shown in the inset exhibits a linear relationship:

Y = –1.3677 + 0.08491X, R^2 = 0.99579, which indicated that the electrochemical kinetics reaction is adsorption-controlled as the adsorption-controlled process should result in a linear plot of I versus scan rate (ν). The linearity was observed over the entire range (50 - 110 mV/s) of scan rates studied with standard deviation value of 0.20232. In LSV, the potential required for the direct oxidation of β –D glucose at CNS electrodes was found to be -0.08 to -0.09 V. The shifting of potentials may be due to the adsorption of oxidised products of β –D glucose on the electrode surface.

Fig. 6 represented the LSV of 10^{-5} M β –D glucose in 0.001M H_2SO_4 (pH ~6.0) at a scan rate of 100 mV/s at bare silver, glassy carbon and CNS electrode. Almost no response in peak current was observed at bare silver electrode indicating that it cannot undergo the reaction in the given potential range. Fig. 6 also showed that though the potential, required for the oxidation of β –D glucose at glassy carbon and CNS electrodes is almost equal (~-0.08 to -0.09 V) but the intensity of peak current was found to be much higher in case of CNS electrode.

3.4 Effect of time interval on the peak current and peak potential of β –D glucose at CNS electrode

Fig.7 showed the 2D and 3D plots of LSV of 10^{-5} M β –D glucose in 0.001M H_2SO_4 (pH ~6.0) at various time intervals (2 to12 min) and at a fixed scan rate of 100 mV/s. Fig. 8 s showed the 2D and 3D plots of SWV of same concentration of glucose in the time interval range of 2-14 minute and at 12 Hz frequency (E_{ampl} = 0.010 V). Calibration plots (in inset) showed a linear dependence of the anodic peak current on the entire range of time interval studied in both cases with correlation coefficient of 0.99849 (Y = 9.76667 + 1.05X), 0.99535 (Y = 5.67136 + 1.89749X) respectively [35,36]. The standard deviation value was found to be 0.24152 for LSV and 0.91575 for SWV. It may be attributed to the fact that as the time was increased, more –OH and –COOH groups were involved in anchoring of the β –D glucose. However, if the study was conducted over an extended time interval range, then a breakdown in the linearity relationship was observed. This may be attributed to the adsorption of oxidized products of β –D glucose on the electrode surface or due to the stabilization of current with time.

3.5 Effect of frequency on the peak current and peak potential of β –D glucose at CNS electrode

Fig. 9 showed the 2D and 3D plots of SWV, which displayed the overlapping of voltagrams of 10^{-5} M β –D glucose at CNS electrode at various frequency rate (7Hz – 12 Hz), maintaining the same pH. For SWV studies E_{step} was 0.005V and E_{ampl} was fixed to 0.010 V. The current versus frequency plot shown in the inset, exhibited a linear relationship, confirming the process to be adsorption controlled. The regression equation of I / μA = 3.67619 + 2.15714 Hz gave R^2 value of 0.99527. Standard deviation value was found to be 0.44051. The potential required for the direct oxidation of the analyte in SWV technique was similar to that of LSV technique (-0.08 to -0.09 V). Therefore, it can be concluded that there was no effect of frequency on the peak potential of the analyte. The intensity of the current was found to increase with the frequency upto 12Hz, but if the study was conducted beyond 12Hz, a breakdown in the linearity relationship was observed. This may be due to the adsorption of oxidized products of β –D glucose on the electrode surface.

3.6. Linearity, detection limit, sensitivity and stability of the non enzymatic β –D glucose sensor

SWV was employed to determine the linearity, detection limit and sensitivity of sensor. Fig.10 (A) showed the plots of SWVs of different concentrations of β –D glucose from 1 to 100 μM in 0.001M H_2SO_4 at a particular frequency of 12 Hz and E_{ampl} of 0.010V. It was observed that the oxidation current increased linearly with the increase of β –D glucose in the range of 1 - 100 μM concentration. The linear regression equation of I/μA = 8.86609 + 2.491 μM gave the R^2 value of 0.99594. For better understanding of the lower detection limit, SWV studies with 0 to 35 μM β –

D glucose was done, maintaining the same operating conditions (Fig. 10 (B)). The inset showed a linear relationship in the mentioned range of concentration showing R^2 value of 0.99574. The lower detection limit was found to be 0.802 μM (S/N =3). The sensitivity was calculated using the slope of the current versus concentration calibration plot (Fig. 10 inset) divided by the active surface area of CNS according to the following equation [37]:

Sensitivity = slope of the plot / active surface area of the electrode , where the active surface area of CNS was 0.0958 cm^2 and the slope was 2.491 μA/μM. The sensitivity of the CNS sensor was calculated to be ~26.002 ± 0.01 μA/μM•cm^2 .

The detection limit, sensitivity and response time of CNS electrode have been compared with those of other reported electrodes used as glucose sensors [22,26-28] (Table 1).

The reproducibility of CNS electrode was determined by SWV (Fig. 11), by fabricating the electrode five times separately, followed by determination of 10^{-5} M glucose. This showed a relative standard deviation (RSD) of 1.43%, demonstrating good reproducibility of CNS sensor. The stability of the sensor was also explored by storing the electrode in air for 15 days. The current response of 10-5M β –D glucose was found to be stable, keeping ~ 95% of its initial intensity.

3.7 Interference

The effects of the presence of some small biomolecules on the current response of 10^{-5} M β –D glucose have been evaluated to describe the selectivity of the reported glucose biosensor. Urea, uric acid, cholesterol, dopamine, fructose, vitamin C, L- alanine, glycine, L-serine, L-phenylalanine, tryptophan and tyrosine have no influence on the current response of CNS

electrode at 12Hz frequency in the potential range from -0.08 to -0.09V. Since sucrose shows interference at high potential, so it did not interfered in the working potential range of -0.08 to -0.09V. Thus, if the electrochemical studies of biosensors can be performed at a particular potential range, which is low enough and suitable to drive the reaction of interest, then interfering signals can be avoided.

3.8 Determination of glucose in real samples

The utility of the proposed method for the non enzymatic detection of glucose in real sample, was tested by determining glucose in human serum sample at CNS electrode. The results were summarized in Table 2. The good recoveries of the samples indicated the successful applicability of the proposed method for the determination of glucose.

4. Conclusions

In this paper, we have described the detection of β –D Glucose by a non enzymatic way using CNS, obtained by pyrolysing a natural carbon source, barley. The fabricated CNS electrode showed high sensitivity, selectivity, strong stability and good reproducibility towards the sample solution of β –D glucose in presence of 0.001M H_2SO_4. Moreover, it exhibited significant electrocatalytic response towards β –D glucose, within a wide linear range of 10^{-4} - 10^{-6} M (1 - 100 μM) along with a low detection limit of 0.802 μM. The sensitivity and selectivity of the CNS electrode towards the oxidation of glucose proved its effectiveness as a non-enzymatic glucose sensor for practical applications. However, the control of the shape and the size of these carbon nano sheets and their dependency on the mechanism of biosensing are still under investigation.

Acknowledgements

Authors are thankful to AICTE, New Delhi for financial support and NEHU, Shillong for characterizations.

References :

[1] A.S.L.Roberto, M.I. Rodrigo , N.C. Frank, Chapter 2 , Nanomaterials for biosensors and implantable biodevices, F. N. Crespilho (ed.), Nanobioelectrochemistry, Springer-Verlag Berlin Heidelberg, 2013. DOI: 10.1007/978-3-642-29250-7_2.

[2] P. M. Ajayan, Nanotubes from carbon , Chem. Rev., 99 (1999) 1787-1800.

[3] N. Parviz, F. Farnoush , L. Bagher , et al., Glucose biosensor based on mwcnts-gold nanoparticles in a nafion film on the glassy carbon electrode using flow injection FFT continuous cyclic voltammetry. Inter. J. Electrochem. Sci., 2010 , 5: 1213 – 1224.

[4] W . Joseph, Electrochemical glucose biosensors , Chem. Rev., 108 (2008) 814-825.

[5] H.Y. Eun , Y.L .Soo, Glucose biosensors: An overview of use in clinical practice –a review sensors, 10 (2010) 4558-4576.

[6] A.P. Turner, B. Chen, S.A. Piletsky, In vitro diagnostics in diabetes: meeting the challenge Clin. Chem.,45 (1999), 1596-1601.

[7] A. Heller , Amperometric biosensors , Curr. Opin. Biotechnol., 7(1996) 50-54.

[8] A. Heller, B. Feldman, Electrochemical glucose sensors and their applications in diabetes management, Chem. Rev., 108 (2008) 2482-2505.

[9] S.B. Bankar, M.V. Bule , R.S. Singhal, et al., Glucose oxidase: An overview, Biotechnol. Adv., 27 (2009) 489-501.

[10] Y. Zhou, L. Wang, Z. Ye, et al., Mango core inner shell membrane template-directed synthesis of porous ZnO films and their application for enzymatic glucose biosensor, Appl. Surf. Sci., (2013), http://dx.doi.org/10.1016/j.apsusc.2013.08.058 (In Press)

[11] A.G. Erik, M. Hemanshu, M. Thomas, et al., Reengineered glucose oxidase for amperometric glucose determination in diabetes analytics, Biosens. Bioelectron., 50 (2013) 84-90.

[12] B. Peng , L. Jing , S.B Anant, et al., Evaluation of enzyme-based tear glucose electrochemical sensors over a wide range of blood glucose concentrations, Biosens. Bioelectron., 49 (2013) 204–209.

[13] Y. Jiao, L. Hyuck, C. Misuk, et al., Nonenzymatic cholesterol sensor based on spontaneous deposition of platinum nanoparticles on layer-by-layer assembled CNT thin film , Sensor Actuat B-Chem.,171 (2012) 374– 379.

[14] F. Li, J. Song, F. Li, et al., Direct electrochemistry of glucose oxidase and biosensing for glucose based on carbon nanotubes@SnO2-Au composite, Biosens. Bioelectron., 25(4), (2009) 883-888.

[15] N. Xiangheng , L.Yuxiu , T. Jie , et al., Electrochemical sensing interfaces with tunable porosity for nonenzymatic glucose detection: A Cu foam case, Biosens. Bioelectron., 51 (2014),22–28.

[16] E. Shoji , M.S. Freund, Potentiometric sensors based on the inductive effect on the pKa of poly(aniline): a nonenzymatic glucose sensor, J. Am. Chem. Soc., 123 (2001) 3383–3384.

[17] C. Serhiy , C. Chan-Hwa, Gold nanowire array electrode for non-enzymatic voltammetric and amperometric glucose detection, Sensor Actuat B-Chem.,142 (2009) 216–223.

[18] J. Wang , D.F. Thomas, A. Chen , Nonenzymatic Electrochemical Glucose Sensor Based on NanoporousPtPb Networks , Anal. Chem., 80 (2008) 997-1004.

[19] Z. Zhuang, X. Su, H. Yuan., et al., An improved sensitivity nonenzymatic glucose sensor based on a CuO nanowire modified Cu electrode, Analyst, 133 (2008),126–132.

[20] S. Park, H. Boo, T.D. Chung, Electrochemical non-enzymatic glucose sensors, Anal. Chim. Acta , 556 (2006) 46–57.

[21] K. Singh , A. Umar, A. Kumar, et al., Non-Enzymatic glucose sensor based on well-crystallized ZNO nanoparticles , Sci. Adv. Mater. 4 (2012) 994-1000.

[22] V. Anithakumary, N.T.E. Mary, J.Divya, et al., Nonenzymatic glucose sensor: glassy carbon electrode modified with graphene- nickel/nickel oxide composite, Int. J. Electrochem. Sci., 8 (2013) 2220 – 2228.

[23] W. Guangfeng, H.Xiuping, W. Lingling , et al. , Non-enzymatic electrochemical sensing of glucose, Microchim Acta, 180 (2013) 161–186.

[24] S.Liu, B. Yu, T. Zhang, A novel non-enzymatic glucose sensor based on NiO hollow spheres, Electrochim. Acta, 102 (2013) 104–107.

[25] H. Fuying , Z. Yanmei, C. Jie , et al., Non enzymatic glucose sensor based on three different CuO nanomaterials, Anal. Methods, 5 (2013) 3050-3055.

[26] X. Zhong, R. Yuan, Y.Q. Chai, In situ spontaneous reduction synthesis of spherical Pd@Cys-C60 nanoparticles and its application in nonenzymatic glucose biosensors, Chem Commun., 48 (2012) 597–599.

[27] B.J. Singh, E. Dempsey, C. Dickinson , et al., Inside/ outside Pt nanoparticles decoration of functionalised carbon nanofibers (Pt19.2/f-CNF80.8) for sensitive non-enzymatic electrochemical glucose detection, Analyst, 137 (2012) 1639–1648.

[28] F. Sun, P. Liu, L. Li , et al., Non-enzymatic glucose biosensor based on Cu/SWNTs composite film fabricated by one-step electrodeposition, Chem Res.Chinese.U., 27 (2011) 1049—1054.

[29] S. Das , M. Saha, Non enzymatic electrochemical detection of glucose at rice starch-nanoparticles modified electrode, Int J Pharm. Bio. Sci., 4 (2013) 967 -975.

[30] S. Das , M. Saha, Preparation of carbon nanosphere from bamboo and its use in water purification, Curr Trends Tech Sci., 2 (2013) 174 – 177.

[31] S. Das , M. Saha, Electrochemical studies of carbon nanotube obtained from coconut oil as non enzymatic glucose biosensor, Adv. Sci. Eng. Med., 5 (2013) 645-648.

[32] S.K. Sonkar, M. Saxena, M. Saha, et al. , Carbon nanocubes and nanobricks from pyrolysis of rice, Jr. Nanosc. Nanotech. 10 (2010) 1– 4.

[33] B. Gebhardt , Z. Syrgiannis, C.Backes , et al., Carbon nanotube sidewall functionalization with carbonyl compounds—modified birch conditions vs the organometallic reduction approach, J. Am. Chem. Soc., 133 (2011) 7985–7995

[34] E.T. Kathryn, G. C. Richard, Electrochemical non-enzymatic glucose sensors: a perspective and an evaluation, Int. J. Electrochem. Sci., 5 (2010) 1246 – 1301.

[35] Y. Lin, F.Lu, Y.Tu, et al., Glucose biosensors based on carbon nanotube nanoelectrode ensembles , Nano Lett. 4 (2004) 191-195.

[36] H.Wang, C. Zhou, J.Liang, et al., High sensitivity glucose biosensor based on Pt electrodeposition onto low-density aligned carbon nanotubes , Int. J. Electrochem. Sci., 3 (2008) 1258-1267.

[37]G. N. Dar, A. Umar, S. A. Zaidi, et al., Ce doped ZnO nanorods for the detection of hazardous chemical, Sens. Actuators B Chem. 173(2012) 72-75.

Scheme-1: Oxidation of β-glucose to gluconic acid

Fig. 1 Images of (A) commercially available standard electrode DS110 (DRP 110CNT) and (B) carbon nano sheet (CNS) modified electrode.

Fig.2 SEM images of carbon nano sheet (CNS)

Fig.3 XRD pattern of carbon nano sheet (CNS)

Fig.4 Raman spectra of carbon nano sheet (CNS)

Fig. 5 2D and 3D LSVs of 10^{-5} M β –D glucose in 0.001M H_2SO_4 at various scan rates (50, 60, 70,80, 100, 110 mV/s) on CNS modified electrode at pH 6.0. Inset: The plot of peak current versus scan rate.

Fig. 6 LSV plots of 10^{-5} M β –D glucose in 0.001M H_2SO_4 at 100 mV/s scan rates on bare Ag electrode , glassy carbon electrode and CNS modified electrode at pH 6.0.

Fig.7 2D and 3D plots of LSVs of 10^{-5} M β –D glucose at CNS electrode in 0.001 M H_2SO_4 in various time intervals (2 ,4 , 6, 8, 10 and 12min) at 100 mV/s scan rate at pH 6.0. Inset : The plot of peak current versus time interval.

Fig.8 2D and 3D plots of SWVs of 10^{-5} M β –D glucose at CNS electrode in 0.001 M H_2SO_4 in various time intervals (2, 5, 8, 10, 12 and 14min) at 12 Hz frequency rate at pH 6.0. Estep = 0.005V and Eampl = 0.010 V. Inset: The plot of peak current versus time interval.

Fig. 9 2D and 3D SWVs of 10^{-5} M β –D glucose in 0.001M H_2SO_4 at various frequency rates (7Hz , 8Hz , 9Hz ,10Hz ,11Hz and 12 Hz) on CNS modified electrode at pH 6.0. Estep = 0.005V and E ampl = 0.010 V. Inset: The plot of peak current versus frequency rate.

Fig. 10 SWV plots at CNS electrode in 0.001 M H_2SO_4 with (A) 1 - 100 μM and (B) 0 - 35 μM of β -D glucose at 12 Hz frequency rate at pH ~ 6.0. Estep = 0.005V and Eampl = 0.010 V. Inset: Calibration curve of response current versus β –D Glucose concentration.

Fig.11 Stability of the responses for 10^{-5} M β –D glucose obtained at five different modified CNS electrodes. (N= 5, RSD = 1.43%)

Figure

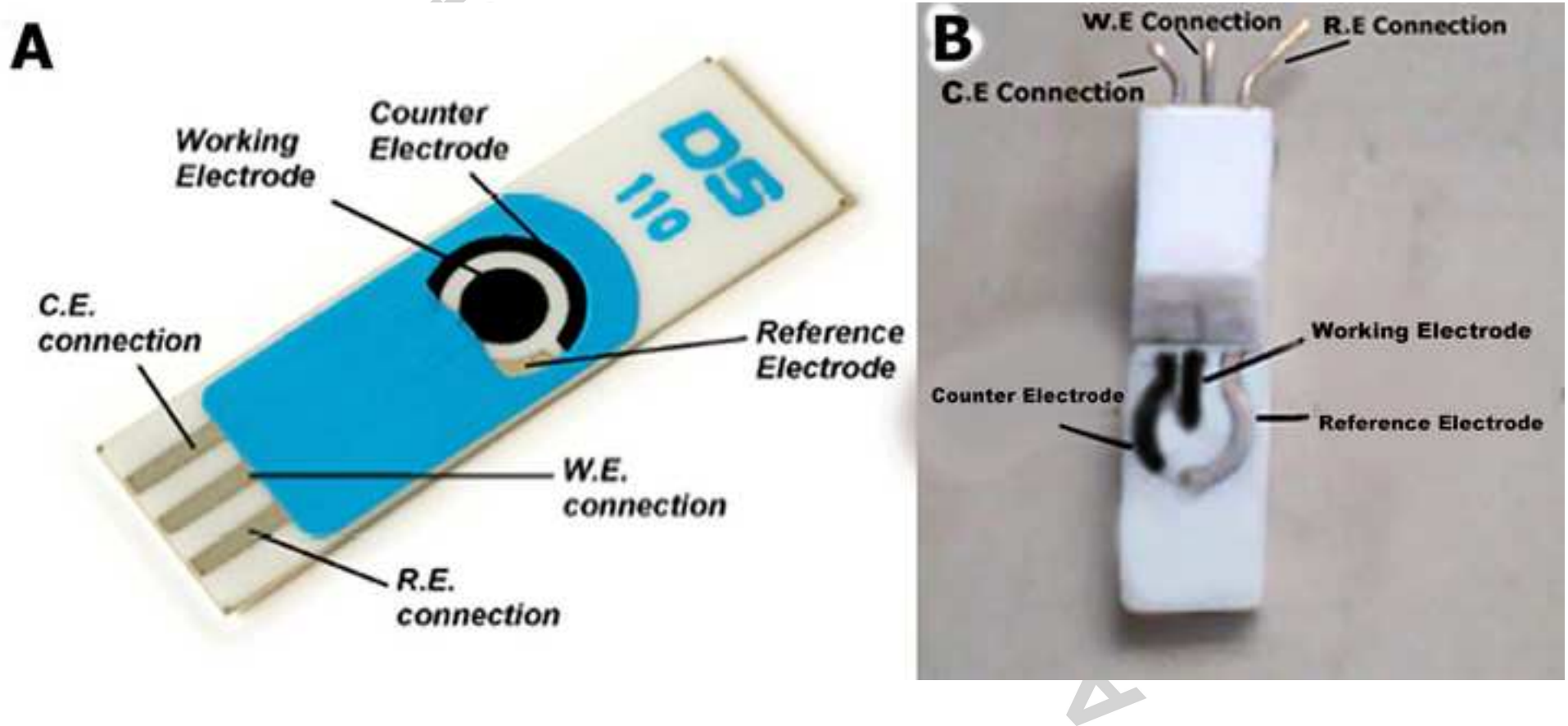

Figure

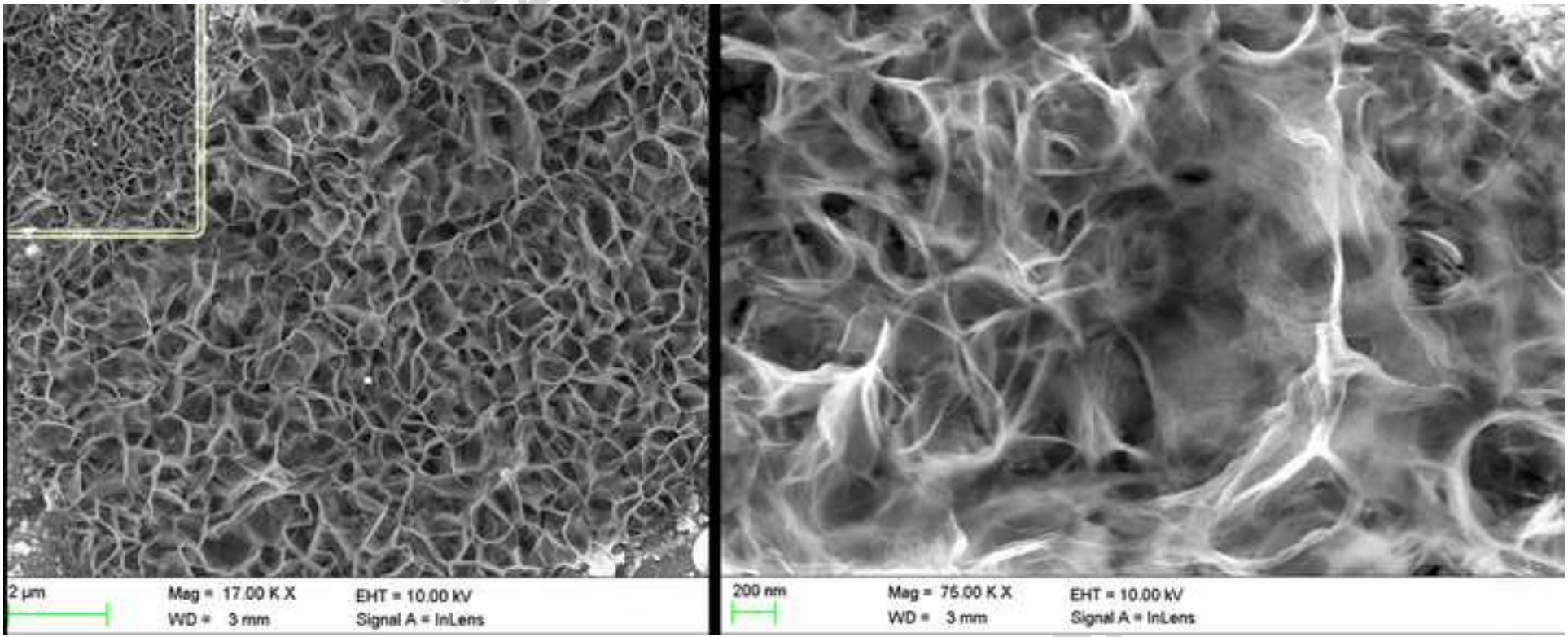

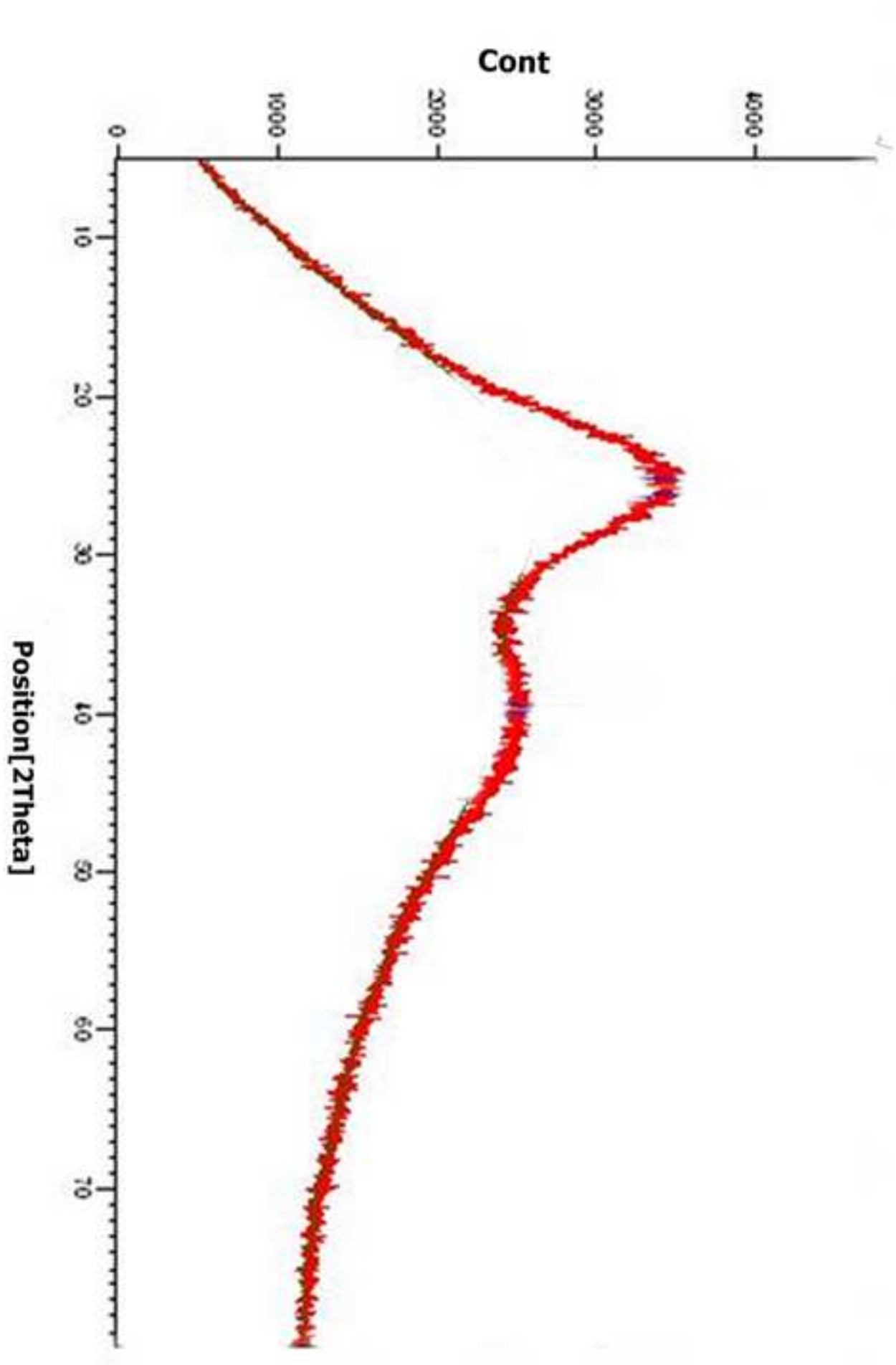

Figure

Figure

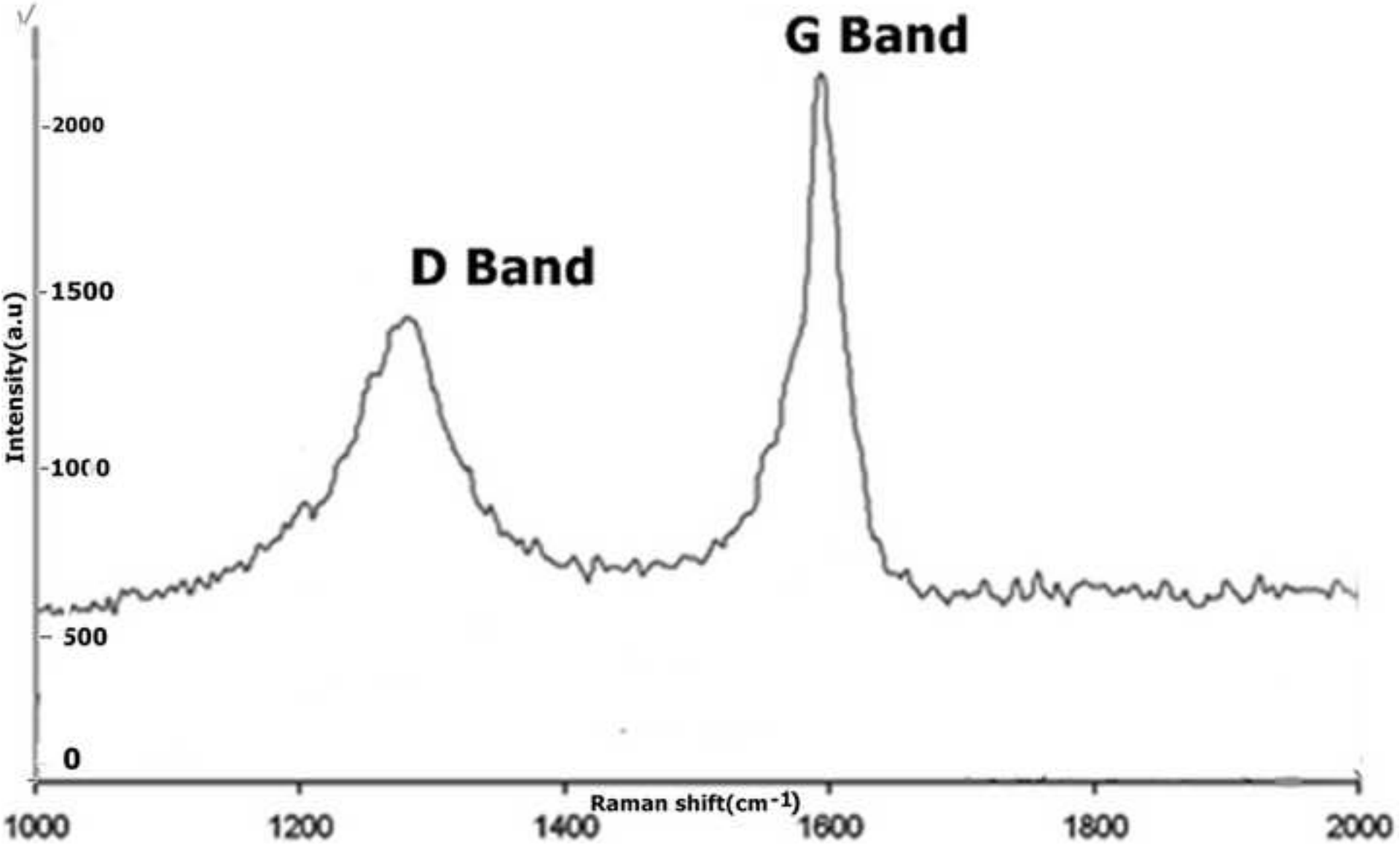

Figure

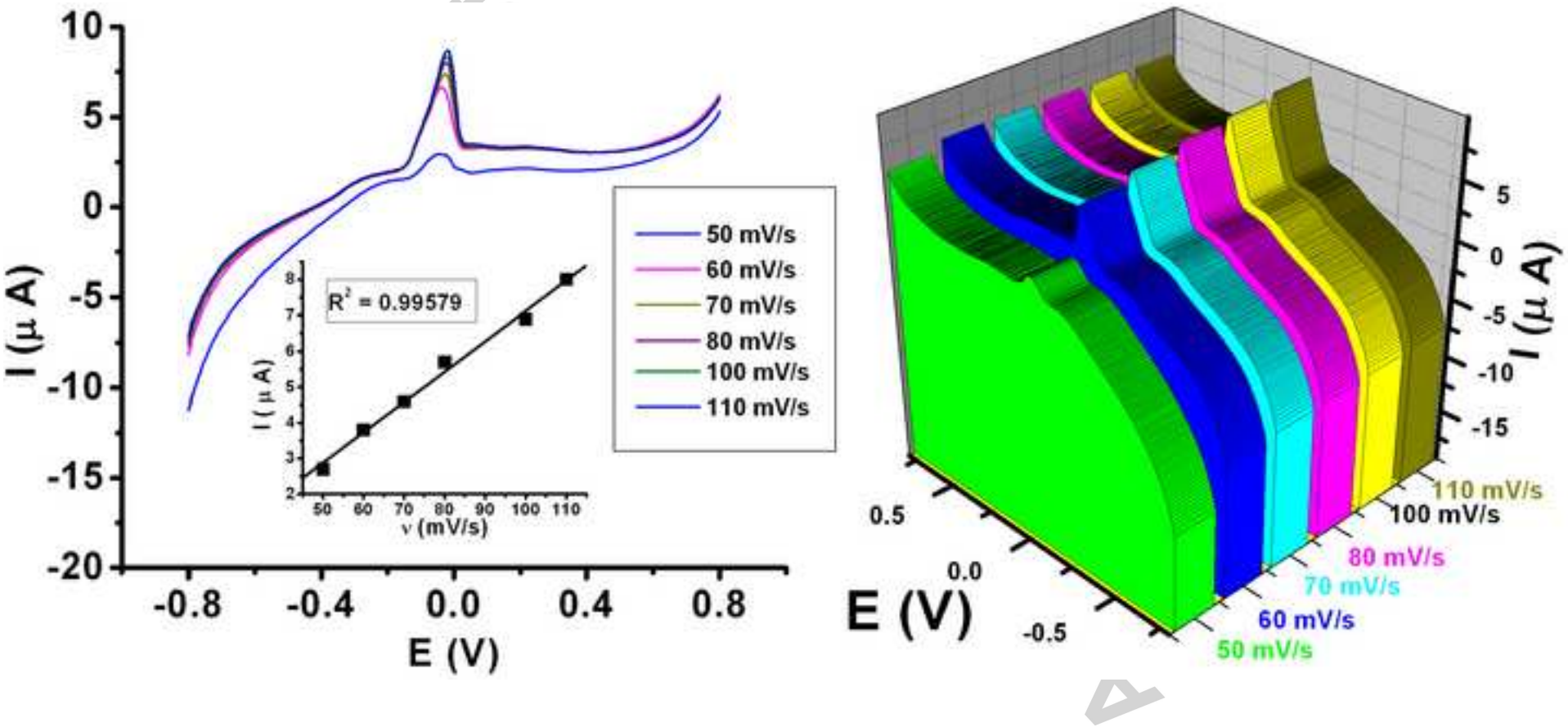

Figure

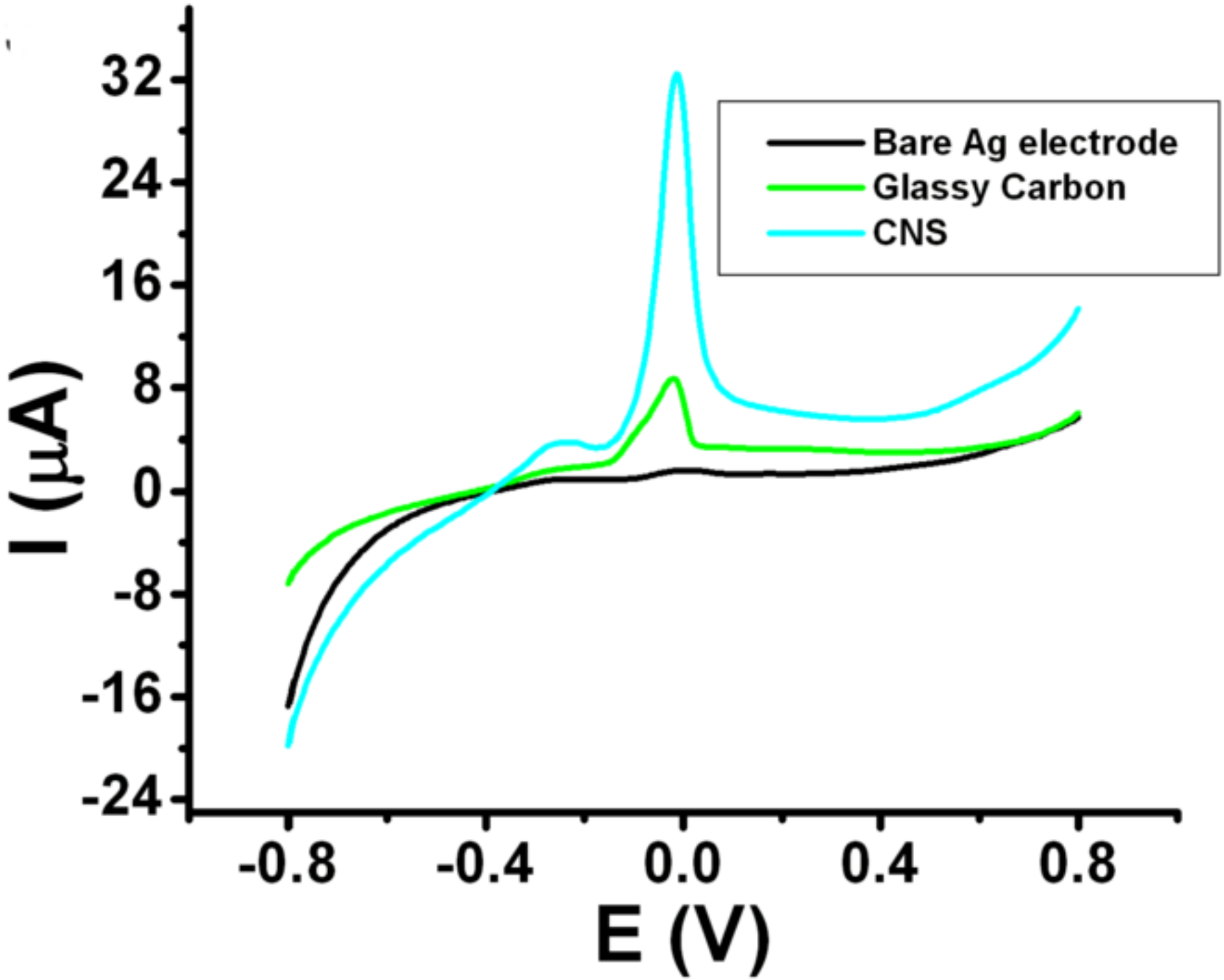

Figure

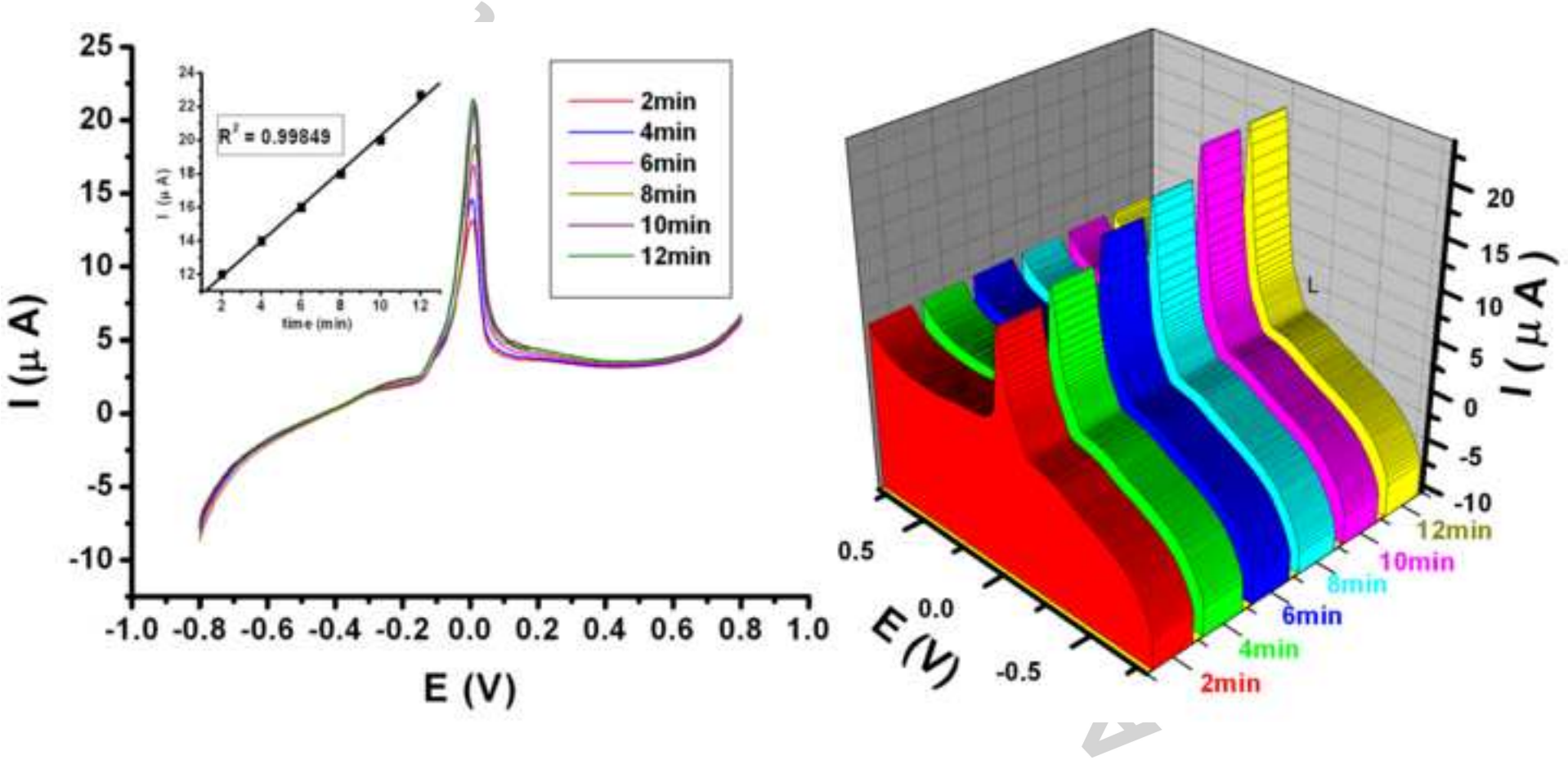

Figure

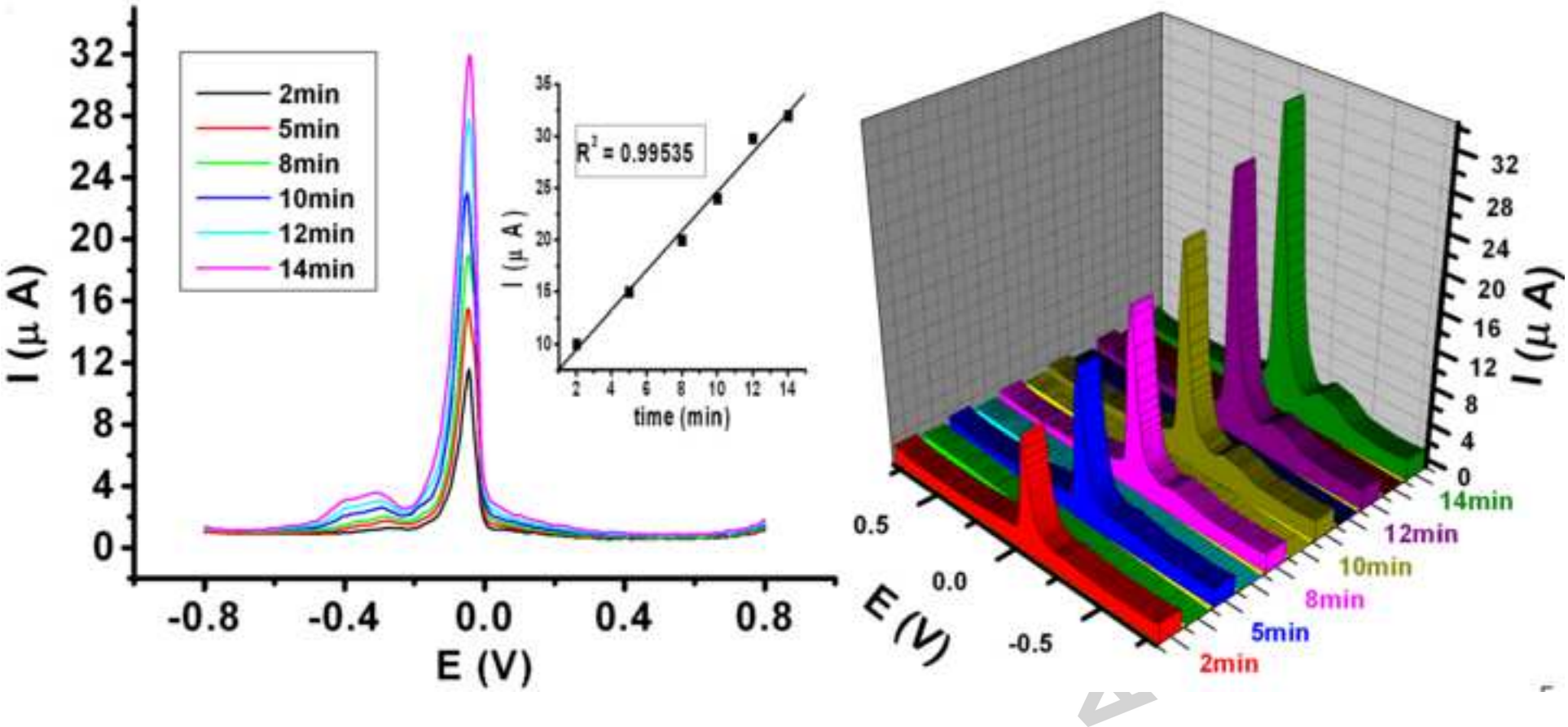

Figure

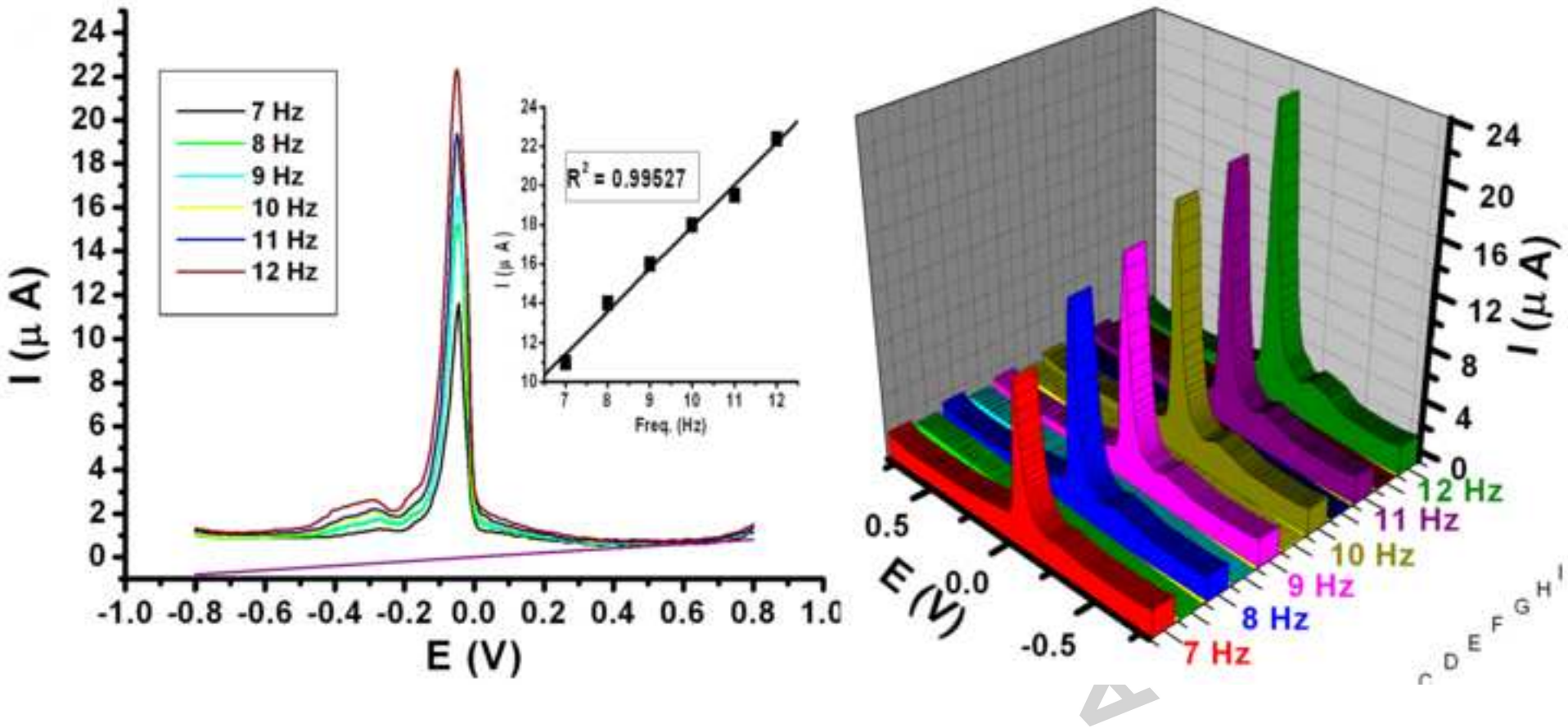

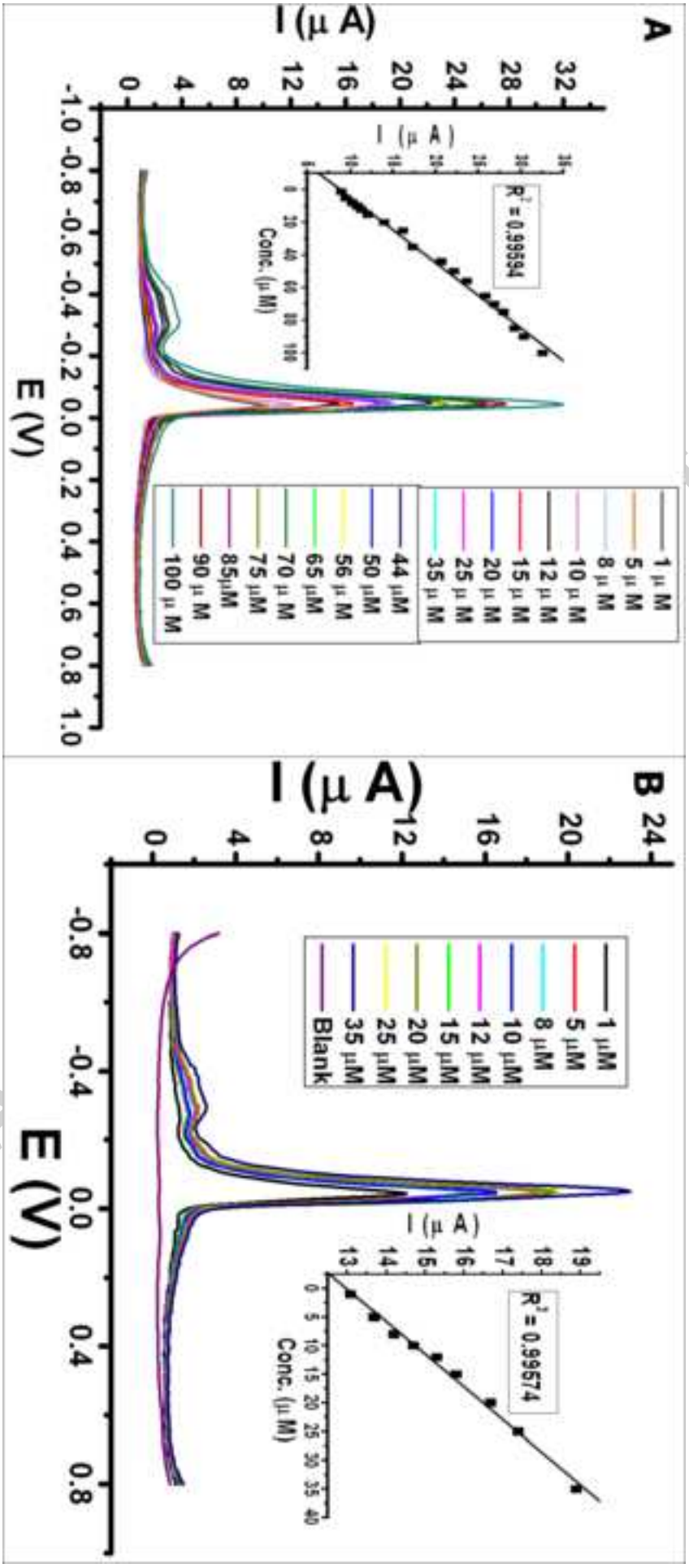

Figure